Susceptibility study of physisorbed oxygen layers on graphite

U. Köbler
Institut für Festkörperforschung (IFF), Kernforschungsanlage Jülich, D-5170 Jülich, West Germany

R. Marx*
Laboratorium für Tieftemperaturphysik Universität Duisburg, D-4100 Duisburg, West Germany
(Received 8 August 1985; revised manuscript received 29 September 1986)

Susceptibility measurements on oxygen (O_2) physisorbed on exfoliated graphite are reported for coverages of up to $\rho=3$. For $0\leq\rho\leq1$ solidification proceeds by one first-order transition at $T'\simeq25$ K associated with a nearly discontinuous decrease of the susceptibility (width about $\Delta T\simeq0.5$ K) and a nearly δ-like anomaly in the specific heat. For the second and higher coverages solidification spreads over a temperature interval as broad as $\Delta T\simeq8$ K. This more intricate solidification process is associated with a nearly linear variation of the susceptibility with temperature. We propose to identify this with a two-phase coexistence region corresponding to the θ phase previously proposed on the basis of low-energy electron diffraction measurements. Specific-heat measurements reveal only the low-temperature limit of the solidification process. On the basis of the present measurements we are able to describe some new structures in the O_2-graphite phase diagram which allow a more consistent view of all of the hitherto known details.

I. INTRODUCTION

In the last few years two-dimensional (2D) O_2 physisorbed on Grafoil or carbon foam (both are graphite modifications) has been very extensively investigated using a variety of experimental methods such as susceptibility measurements,[1,2] neutron diffraction,[3] x-ray diffraction,[4,5] low-energy electron diffraction (LEED),[6] and specific heat.[7–9] 2D O_2 receives particular interest since the O_2 molecules form the only known gaseous system having a magnetic ground state. The spin of the O_2 molecules can in turn be used as a probe for the evaluation of the 2D phase diagram. This phase diagram is richly structured and reveals many interesting phenomena such as melting lines and phase boundaries corresponding to magnetic transitions.[9] Moreover not only phase boundaries of crystalline but also of combined crystalline and magnetic origin can be expected. It is however not clear whether or not the magnetic interactions between the O_2 moments do play any role in the melting process of the 2D O_2 film. Comparison with three-dimensional 3D oxygen shows that solidification does not imply an orientational order of the O_2 moments.[10,11] Within the rhombohedral β phase and the cubic γ phase of 3D bulk oxygen no magnetic long-range order does exist. The monoclinic low-temperature α phase does, however, show an antiferromagnetic order. It appears that the magnetic order is a consequence of the structural order such that the magnetic ordering does require the α-type lattice structure with the extrapolated Néel temperature falling into the magnetically disordered β phase.

Some details of the O_2-graphite phase diagram are now well understood but others are still a matter of controversy, for instance the character of the melting transition at $T''\simeq32$ K. A careful specific-heat study of the melting lines[12] revealed at $T'\simeq25$ K symmetrical anomalies which are reminiscent to blurred δ anomalies. At T'', however, λ-like anomalies are observed, the shape of which points to some real energetic structure of the transition. The δ anomalies can conclusively be associated with one broadened first-order transition but one adequate and most simple interpretation of the λ anomalies would be to assume the existence of just two closely spaced nonresolved phase transitions. This interpretation is supported by the observation of a broad double structure in the specific-heat anomaly within a narrow coverage interval around $\rho\simeq1$ (note that all coverages are given in units of the density of a hypothetical $\sqrt{3}$ structure).

It is interesting to note that just for the particular coverage of $\rho\simeq1.8$ melting produces virtually no anomaly either in the susceptibility nor in the specific heat.[2] We must conclude that here solidification becomes a smooth process by which the liquid and the solid phase assume very similar properties such that no marked change does occur for $\rho\simeq1.8$ at the melting point itself.

One particular point of interest in the O_2-graphite system is the possible existence of magnetic 2D ordering transitions. Although a magnetic ordering at the melting transition can be ruled out, an antiferromagnetic order has been observed with neutron scattering techniques below $T\simeq12$ K for $\rho>1.7$.[3] Recent specific-heat measurements[8,9] could confirm the existence of a transition at $T\simeq12$ K but like the α-β transition of 3D solid oxygen, it is plausible to assume that this transition is driven by crystallographic degrees of freedom with the magnetic order being enabled only after the lattice transformation. Unfortunately the magnetic susceptibility is of little help in characterizing the nature of this transition since once the 2D film is in the solid phase the susceptibility is very small and transformations from one solid phase into another change the susceptibility very little. One further particularity of the susceptibility is that although it reacts

very sensitively to the 3D gas-liquid transformation it does exhibit no anomaly for this transition in two dimensions. The only phase transitions seen by this method are those into states with solidlike properties.

The motivation for the present investigation is to explore the different melting phenomena described above in more detail with the aid of susceptibility measurements. It is hoped that this method may contribute to the solution of the problem of which nature the above-described melting processes belong and that it will give further information about the details of 2D O_2 melting. One may ask for the physical mechanism that in the present case melting can also be detected in a susceptibility experiment. Note that there is weak coupling to the molecular axis of the resulting spin $S=1$ of the two outer electrons of the O_2 molecule. This coupling has its origin in a combination of spin-spin and spin-orbit couplings.[14] At a liquid-to-solid phase transition the rotational degrees of freedom of the O_2 molecule freeze and this is noted by a decreasing susceptibility. As a consequence, there should be a sensitive response in the temperature dependence of the susceptibility $\chi(T)$ to melting. At first-order melting a discontinuous decrease of $\chi(T)$ at T_m is anticipated when going from the liquid to the solid state, while at second-order melting a continuous decrease at T_m should be seen. A finite and weakly temperature-dependent susceptibility can be expected if the magnetic moments are locked into fixed orientations like it is given for a state with an antiferromagnetic spin order. It must, however, be noted that a real discontinuous $\chi(T)$ dependence is not observed at all in our experiments. Presumed first-order transitions are always smeared out over a finite-temperature interval typically of the order of 0.5 K. This may partly be explained by substrate inhomogeneities and coherence length limitations due to finite grain dimensions of the substrate. Therefore, there exists no sharp transition temperature and melting is completed only after a finite-temperature increment.

II. EXPERIMENTAL PROCEDURE

All susceptibility measurements are performed in the closed cell configuration. Samples are prepared by sealing small sheets of Grafoil (a graphite modification of high specific surface and well-defined adsorption planes[15]) under a definite O_2 pressure into quartz containers. The accurate O_2 content has been controlled after the measurement by breaking the quartz containers off in a vacuum vessel with a calibrated volume and measuring the absolute pressure rise. The O_2 content is expressed in units of one commensurate $\sqrt{3}\times\sqrt{3}$ monolayer O_2 by assuming that 1.35×10^{20} O_2 particles result in one monolayer for a 1-g sheet of Grafoil. Note that although this commensurate structure is not realized in case of adsorbed O_2, the normalization to ρ_0 is nevertheless useful, because on the basis of this definition the monolayer of in-plane molecules is complete at $\rho=\rho_0$.

The susceptibility measurements presented here are all made with a field of 0.5 T applied perpendicular to the Grafoil sheet. For this geometry one must be aware that the spin system may undergo a field-induced change from an in-plane orientation into the energetically more favorable orientation parallel to the field, viz., perpendicular to the Grafoil sheet. Moreover, such a change in orientation could be associated with a phase transition. Therefore, we varied the field in the range $0.1<B_0<1$ T but identical susceptibility results were obtained apart from small shifts in the critical temperature normally smaller than 1 K. A field of 0.5 T can therefore be considered as a small perturbation which does not induce dramatic changes in the spin order so that field zero properties are sampled.

For the susceptibility measurements with the force method after Faraday the quartz containers are suspended by a thin copper wire and positioned into the center of a superconducting coil system consisting of one dipole coil for field generation and one quadrupole coil for an independent generation of the field gradient. Note that the numerical values of the susceptibility are given in SI units and are hence larger by a factor of 4π as compared with cgs units.

III. RESULTS: IMPLICATIONS FOR THE O_2-GRAPHITE PHASE DIAGRAM

As a reference for the following adsorption investigations in Fig. 1 we show the temperature dependence of the magnetic susceptibility of pure oxygen measured on a closed quartz container without Grafoil inside it. In the high-temperature gas phase ($T>70$ K) the susceptibility follows the anticipated Curie law $\chi=C/T$ with a Curie constant C which does correspond to an effective magnetic moment per O_2 particle of $\mu^2=7.9\mu_B^2$. This value is very close to the theoretical one for a pure spin moment with $S=1$ and $g=2$.

At $T\simeq70$ K the gaseous oxygen transforms into a liquid which is noted by a sharp susceptibility maximum. This is in contrast to the 2D situation where the gas-

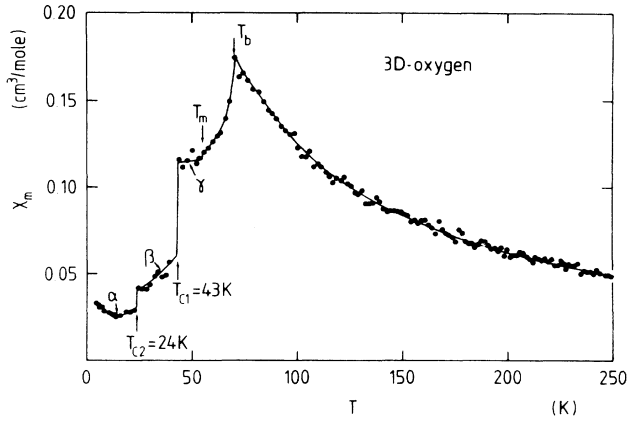

FIG. 1. Temperature dependence of magnetic susceptibility of 3D oxygen measured in a closed quartz cell without graphite. The χ maximum notifies the boiling point T_b. Melting at T_m is associated with only a weak χ anomaly but the two further phase transitions of 3D solid oxygen from $\gamma\rightarrow\beta$ and $\beta\rightarrow\alpha$ phase are clearly revealed by strong discontinuities.

liquid transformation does produce no anomaly in the susceptibility. The observed boiling point at $T_b \simeq 70$ K is smaller than the normal value of 90.2 K since the estimated pressure in the quartz cell is only 80 Torr at $T=70$ K. In the liquid phase the susceptibility decreases with decreasing temperature and solidification at $T_m \simeq 54.8$ K is associated only with a very small susceptibility anomaly. This is again in contrast to the 2D situation where the susceptibility of the liquid does continue to increase with decreasing temperature. As is well known,[16,11] solid 3D O_2 undergoes two further phase transitions of first order at approximately 44 and 24 K which are clearly revealed by Fig. 1. This agreement with previous investigations on 3D solid oxygen shows that the amount of oxygen in our samples is sufficient to result in a solid with 3D properties. If we assume a homogeneous wetting of the inner surface of the quartz container an O_2 film having a thickness of 10^3 atomic layers will be formed.

The $\chi(T)$ results in Fig. 1 depart considerably from the behavior reported in Ref. 11 for the liquid phase $55 < T < 70$ K. Here the results depend much on the experimental conditions and are not very reproducible even for measurements with the same experimental equipment. In our case the experiment is conducted for a constant particle number but with an increasing pressure as a function of increasing temperature. $\chi(T)$ increases strongly in the liquid phase on approaching the boiling point. This is in contrast to the zero-pressure measurements reported in Ref. 11 which show a slightly decreasing susceptibility on approaching the boiling point probably because of a loss in particle number due to evaporation.

On adding Grafoil to the quartz container the free surface enlarges by approximately a factor of 10^3. Very reproducible results are obtained for $\chi(T)$ and the disappearance of the phase transitions characteristic for 3D oxygen shows that practically all oxygen is physisorbed by the Grafoil.

Figures 2(a)–2(c) display three typical susceptibility curves for coverages of $\rho=0.84$, 1.52, and 2.50. Susceptibility contributions coming from the quartz container and the Grafoil sheet are subtracted as temperature-independent proportions. This is approximately correct for the temperature range $20 < T < 60$ K. Below $T \simeq 20$ K the susceptibility of both quartz and Grafoil becomes more paramagnetic and this is seen for all $\chi(T)$ curves in Fig. 2 as a susceptibility rise at temperatures below $T \simeq 20$ K. Note the different ordinate scales for the different samples.

Apart from the different slopes on the low-temperature side of the $\chi(T)$ maximum the qualitative aspects of the three $\chi(T)$ curves are not so different and suggest that essentially the same type of transformation does happen in the O_2 film which, however, proceeds under modified conditions for different O_2 densities. The associated physical process giving rise to a reduced susceptibility in the low-temperature phase is clearly a solidification as has been verified by neutron and x-ray diffraction methods.[3–5] On the high-temperature side all curves show an approximate Curie-Weiss behavior with increasing susceptibilities for decreasing temperatures. In particular the $\rho=0.84$ sample does not show any anomaly near

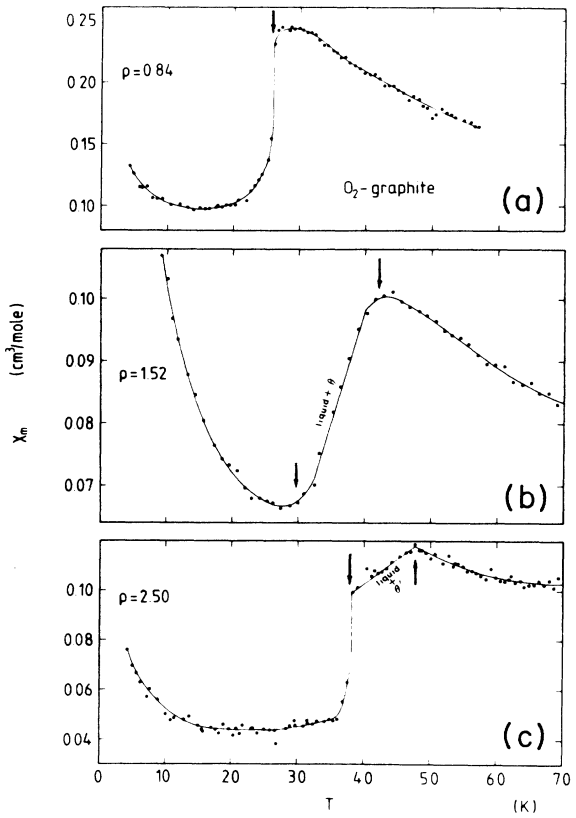

FIG. 2. Susceptibility as a function of temperature for three O_2-graphite samples with different coverage ρ. On the high-temperature side of the χ maximum the susceptibility does obey an approximate Curie-Weiss law with negative paramagnetic ordering temperatures. Solidification is noted as a decrease in susceptibility with decreasing temperature and is associated either with a nearly discontinuous decrease of χ ($\rho=0.84$) (a) or it involves two-phase coexistence regions ($\rho=1.52$ and 2.50) [(b) and (c)] with a nearly linear variation of χ as a function of temperature. For phase notations see Fig. 5.

to $T \simeq 50$ K where the gas-to-liquid transformation occurs according to the isothermal vapor pressure experiments.[17] As is well established this high-temperature phase must be identified either with the 2D liquid or the 2D vapor phase or the coexistence of both which all differ markedly from the 3D liquid phase by showing an increasing susceptibility with decreasing temperature, whereas the susceptibility of the 3D liquid decreases with decreasing temperature (refer to Fig. 1). While for the 3D liquid the steric rotations become increasingly hindered with decreasing temperature due to an increasing viscosity, the 2D liquid seems to experience a temperature-independent hindering potential resulting in a Curie-Weiss law of susceptibility. It is interesting to note that the temperature at which the oxygen gets adsorbed on the graphite surface ($T \simeq 63$ K) cannot be identified from the $\chi(T)$ curves. Although measurements of the 3D vapor pressure as a function of temperature reveal a sharp drop of pressure at the tem-

perature where physisorption takes place ($T \simeq 63$ K), the susceptibility is not much affected by this condensation process. This means that the magnetic moments of the oxygen molecules are nearly as free to rotate in the adsorbed liquid phase as they are in the three-dimensional gas state. The adsorption process does therefore not involve the rotational degree of freedom since otherwise a dramatic effect should be observed in the susceptibility. For the magnitude of the above discussed 2D hindering potential we may draw the conclusion that it is not only weakly temperature dependent but it must be a very weak potential as well at least for small coverage numbers.

Next we discuss the results displayed in Figs. 2 in detail. The $\rho = 0.84$ sample shows a sudden decrease of susceptibility at $T' = 25$ K. This phase transition occurs at a constant temperature for the coverage range $0 \lesssim \rho \lesssim 0.85$ and belongs to those details of the O_2-graphite phase diagram which can be regarded as being well established. It corresponds to the triple-point line between the 2D solid δ phase and the 2D liquid phase both in equilibrium with 2D gas. The solid phase is an incommensurate phase of O_2 molecules which have their axes oriented in parallel with the adsorption plane.[4–6] In order to estimate the character of the phase transition at T' more accurately we show in Fig. 3 an example for the behavior of $\chi(T)$ with a considerably increased temperature resolution. It can be seen that although $\chi(T)$ is continuous it decreases strongly within a narrow temperature interval of $\Delta T \simeq 0.5$ K. This is in accordance with specific-heat measurements [one example is shown in Fig. 4(a)] having a width of the same order. The specific-heat measurements reveal symmetrical peaks at a T' which is common to all peaks. We take therefore the results of both methods as an indication for a first-order transition smeared out by secondary effects like substrate inhomogeneities[18] and finite-size effects.[19] Moreover, the constant temperature of the heat-capacity peak points to a liquid-gas-solid triple-point line. This is in agreement with the interpretation of former measurements which postulate an island formation of the δ phase embedded into a surrounding gaseous phase.[8,20] The triple-point structure means that there is δ + gas coexistence below $T' = 25$ K and liquid + gas coexistence above $T' = 25$ K.[5]

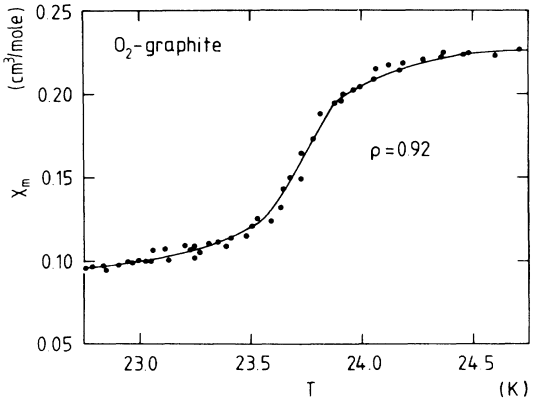

FIG. 3. Temperature dependence of the susceptibility in the vicinity of the $\simeq$25-K melting transition ($\rho < 1$) shown with a considerably increased temperature resolution. A presumed first-order melting transition is never observed as a real discontinuity of $\chi(T)$.

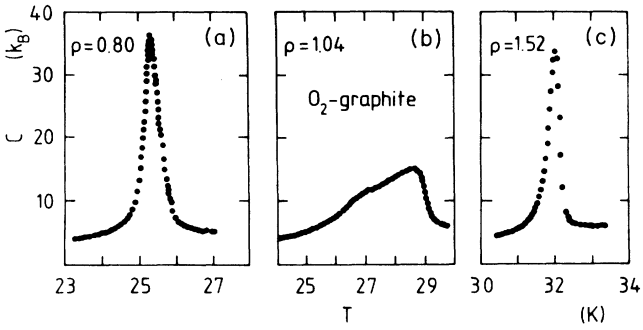

FIG. 4. Specific heat of 2D O_2 per particle in units of k_B as a function of temperature T (Ref. 12). The $\rho = 0.80$ (a) anomaly reflects a blurred first-order transition from the solid δ phase to the liquid phase. For a discussion of the λ anomalies ($\rho = 1.04$ and 1.52) [(b) and (c)] refer to text.

For the coverage range $1 < \rho < 2$ the specific heat and the susceptibility give results which at first glance seem to display partial disagreement. A few percent above the coverage $\rho = 1$ the specific heat shows broad and structured anomalies [Fig. 4(b); $\rho = 1.04$] but for coverages of $\rho > 1.06$ it shows pronounced λ anomalies [Fig. 4(c); $\rho = 1.52$]. The susceptibility at $\rho = 1.52$ [Fig. 2(b)] shows a broad temperature region where it is a linear function of temperature. This temperature interval is however much too large to be explained with the just given inhomogeneity arguments. If we identify the two ending points of the linear χ portion with phase transitions ($T_{\text{start}} = 32$ K, $T_{\text{end}} = 40$ K for $\rho = 1.52$) we obtain good agreement with the specific heat as regards the position of the lower phase transition but at the higher phase transition no measurable specific-heat anomaly can be observed.

A linear $\chi(T)$ dependence is normally characteristic for a two-phase region with a linearly varying proportion of both components as a function of temperature (so-called lever rule). What is the nature of this two-phase region? From the susceptibility measurements it is clear that one of these phases does have liquidlike properties while the other one does have nearly solidlike properties. This is because the susceptibility does not decrease further below $T_{\text{start}} \simeq 32$ K, e.g., it has assumed the T dependence typical for the solid state. Specific-heat measurements, on the other hand, reveal a phase transition at $T \simeq 32$ K and therefore the second phase of this two-phase region cannot be identical with the solid phase. As a remedy of this problem we identify the second phase with the θ phase observed in LEED experiments[20] and propose that this phase has properties characterized by a largely decreasing mobility of the O_2 molecules with decreasing temperature. It is tempting to speculate that the θ phase has liquid-crystal-like properties with the axes of its molecules being

smectic-crystal-like ordered, e.g., but with their centers being disordered in the 2D plane. Note that the structure of the δ phase is such[6] that the theory of dislocation-mediated melting for anisotropic layers of molecules considered by Ostlund and Halperin and other authors should be applicable.[13] This theory suggests that such layers may pass through smecticlike phases. That theoretical statement would support our assumption; however, we concede that at present there are no other experimental evidences which would support our hypothesis. In Ref. 20 it is stated that the δ phase melts into a phase distinctly different from a liquid which on the other hand does not have solidlike properties. That phase is named the θ phase. We believe that the phase discussed here is identical with that θ phase and therefore the corresponding region is called the θ phase (Fig. 5). The boundaries of this phase cannot be given very precisely because this intermediate phase has properties very similar to the adjacent phases along its boundaries. One consequence of this interpretation is to postulate the existence of one further phase transition from the θ phase to solid. This transition can give only very small anomalies in the susceptibility and the specific heat as well since the properties of a solid and the θ phase should be very similar. From this similarity it follows further that the temperature interval over which the solid and the θ phase can coexist should be narrow.

Although the susceptibility measurements do not give any indication for a double structure of the $T\simeq 32$ K anomaly the observed λ anomaly in the specific heat is consistent with a nonresolved sequence of two closely spaced phase transitions. The λ-like rise at the low-temperature side of the specific-heat signal can be interpreted as due to an additional weak phase transition playing the role of a predecessor of the genuine solid-liquid phase transition at $T''=32$ K. Both transitions result by superposition into the observed λ-like shape of the $T''=32$ K anomaly. Although this conclusion is somewhat hypothetical it is consistent with the broad and structured specific-heat results observed only near to $\rho\simeq 1$ [refer to Fig. 4(b), $\rho=1.04$]. It is clear from Fig. 5 (refer also to the discussion of the phase diagram below) that just for $\rho\simeq 1$ a complicated specific-heat structure may result with a tail on the low-temperature side.

It is still a puzzle why the specific heat is sensitive only to the $\delta\rightarrow$liquid transition but not to the $\theta\rightarrow$liquid transition. Note that along the upper existence limit of the liquid $+\ \theta$ phases only partial conversion liquid$\rightarrow\theta$ takes place. On the other hand the relative proportion of the θ component seems to increase with decreasing temperature and this is seen as a decreasing susceptibility. The susceptibility has the advantage of being sensitive to the content of the θ component as a function of temperature while the specific heat is sensitive to the conversion rate, which is low because the total $\theta\rightarrow$liquid conversion spreads over a considerable temperature interval. However, the θ phase itself must have very unusual properties as a function of temperature. We must assume that it is a true intermediate liquid phase in the sense that the viscosity does increase strongly with decreasing temperature.

The $\chi(T)$ curve of the $\rho=2.50$ sample in Fig. 2(c) has again some qualitative similarity with the $\chi(T)$ curve of the $\rho=0.84$ sample but all structures have shifted to larger temperatures. For $\rho=2.50$ also a linear $\chi(T)$ portion is observed, however in the temperature interval $38<T<48$ K (marked $\theta'+\zeta$). This can again be interpreted along similar lines as above as a two-phase coexistence region. Note that in Fig. 5 the corresponding region "$\theta'+\zeta$" and the region "liquid $+\ \theta'$" are reminiscent to the η phase and the fluid II(?) phase, respectively, of Fig. 3 in the paper of Heiney *et al.*[5] These authors suppose that the η phase could either be a separate phase or a coexistence region between a "higher-temperature fluid," which they label fluid II(?) in Fig. 3 of Ref. 5, and the ζ phase. On the basis of the present results we believe this assumption is true, and we may speculate that the "higher-temperature fluid" has similar properties as the previous θ phase. Therefore, we have called it "θ'". We admit, however, that the only experimental evidence for that assumption are the qualitatively similar courses of the susceptibilities depicted in Figs. 2(b) and 2(c) and labeled by liquid$+\theta$ and liquid$+\theta'$ for $\rho=1.52$ and 2.50, respectively. This speculation finds no support by Fig. 6 of Ref. 20 for instance, since here the corresponding phase regions are identified as "fluid(?)". Finally we mention the phase labeled "fluid I" in Fig. 3 of Ref. 5 is certainly identical with our liquid phase.

One particular result with the susceptibility curves for samples having $\rho>2$ is that only a minute change in slope can be seen at $T\simeq 12$ K where the system should undergo a magnetic ordering transition.[3] The existence of a phase transition at $T\simeq 12$ K is well established by neutron diffraction[3] as well as specific-heat measurements.[12] The magnetic susceptibility reacts very sensitively on the melting process but once the adsorption system is in the solid state the susceptibility is no longer very sensitive against further phase transformations. This contrasts with the first-order transformations of 3D O_2 which manifest as pronounced $\chi(T)$ discontinuities. Anyhow, the weak change in slope of $\chi(T)$ at $T\simeq 12$ K does not have the character of an antiferromagnetic transition.

Figure 6 gives an example for $\chi(T)$ of a sample from the third molecular layer ($\rho=3.8$). Also in this case it becomes clearly evident that melting ($\zeta\rightarrow$liquid) does involve three consecutive phase transitions corresponding to the three consecutive phase boundaries at $\rho=3.8$ of Fig. 5.

Combining all critical temperatures observed in the $\chi(T)$ measurements with the specific-heat results as well as considering the known neutron scattering[3] and x-ray data[4,5] we are led to complete the O_2-graphite phase diagram in such a way as is proposed by Fig. 5. The existence of two types of liquids constitutes an important new detail. In other parts, however, the phase diagram gives a more conclusive view of features which were already known.

The growth mode of physisorbed oxygen on graphite is type 2 that means O_2 shows incomplete wetting.[21,22] Henceforth a more appropriate name for the abscissa would be "filling" rather than "coverage;" O_2-graphite coverage 1,2,3,... does not mean monolayer 1,2,3,.... The δ and ζ phases actually are both phases of the first monolayer. At fillings larger than 3 also a second layer may occur.[23] Increase of the filling for the present system

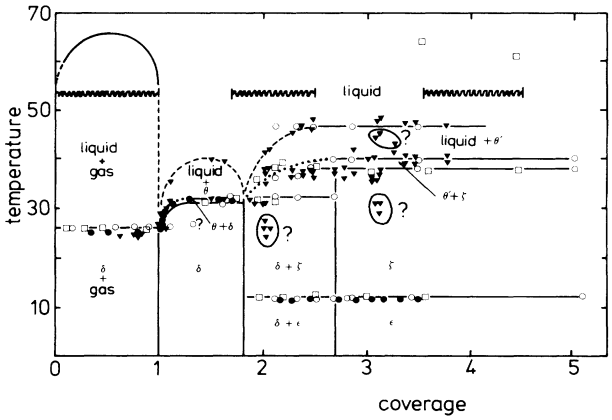

FIG. 5. Synoptic phase diagram for the oxygen-graphite adsorption system collecting all experimental details as they have become available to the authors: (a) the solid lines (with the exception of the dashed lines which have been in part added by the present authors) are due to Fain *et al.* (Ref. 20) [the "ramp" in the midst of Fig. 6 of Ref. 20 has been replaced by a horizontal and a convex phase boundary for $(1 \leqq \rho \leqq 1.8)$ and $(1.8 \leqq \rho \leqq 2.5)$, respectively, since these two phase lines describe the present results much better than the former "ramp" did. Moreover, the assumption of two lines is not in contradiction with earlier experimental results; refer to Fig. 2 of Ref. 8, e.g.]; (b) the open circles are due to Stoltenberg *et al.* (Ref. 8), Stephens *et al.* (Ref. 4), and Heiney *et al.* (Ref. 5); (c) the open squares are due to Awschalom *et al.* (Ref. 2); (d) the solid circles are due to Marx *et al.* (Refs. 7, 9, and 26) and due to unpublished work of one of the present authors (R.M.); (e) triangles mark measurement points due to the present work; (f) hatched lines indicate isothermal vertical rises (Refs. 4 and 5); (g) the dashed line $(0 < \rho < 1.0)$ with a critical point at $T_{2c} \simeq 65$ K on top of the curve represents the boundary between liquid-gas coexistence and the pure gaseous phase (Refs. 5 and 17). Note that all 3D features as reported by different authors (Refs. 8 and 2) have been omitted for more clarity. The existence of the θ phase was first detected by Fain *et al.* (Ref. 20). Used graphite substrates: natural single crystals (Ref. 20), *ZYX* (Refs. 4 and 5), foam (Ref. 5), Grafoil (Refs. 7, 8, 2, and 9), and this work. Note the congruency between the various investigations on different substrate modifications: for instance refer to $\rho = 1$, $T = 26$ K (cross point of four phase boundaries) and to $\rho = 1.8$, $T = 32$ K (cross point of five phase boundaries). The existence and location of the dashed and dotted phase boundaries is speculative. In particular the dotted phase boundaries between the $\theta + \delta$, the $\theta' + \zeta$ equilibrium and the liquid $+ \theta, \theta'$ equilibrium are assumed to be temperature dependent. According to thermodynamics (triple lines are always temperature independent) either the phase equilibrium does not extend below $\rho = 1.2$ and $\rho = 2.7$, respectively, or the course of the dotted lines is erroneous. The aim of future work must be to improve the understanding of the precise location of these phase boundaries. The three clusters of crosses and the one open circle which have question marks do not fit into the present phase diagram. We think these points are in error because of problems with the precise determination of the actual oxygen contents of the sample containers. Narrow first-order coexistence regions are not shown (Ref. 20).

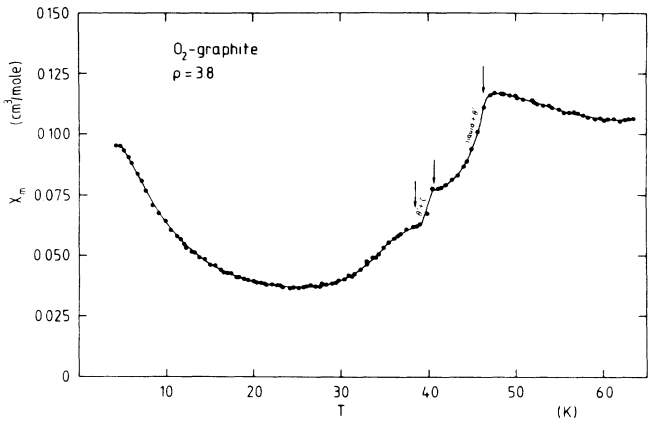

FIG. 6. Temperature dependence of susceptibility for a sample with $\rho = 3.8$. Solidification is accomplished after three phase transitions, involving the isotropic liquid, the θ, θ' phases and the corresponding solid phases δ and ζ, respectively.

means increasing the spreading pressure within the film plane. This pressure (besides the molecules's interactions with the substrate) rules the intensity and kind of interaction (long-range, short-range, antiferromagnetic, etc.) of the adsorbed molecules, their lattice parameters, their orientation with respect to the substrate and the kind of phases observed in the film. Note that Etters and Duparc are able to explain the distortion and antiferromagnetic ordering of the ϵ phase without assuming this phase is a double layer.[24]

It is also believed that the real coverages are falsified by alternate-site adsorption, clustering, and/or intergranular condensation.[23] Therefore, the coverage is subject to considerable uncertainty. For instance, the structural density of the δ phase as observed by LEED and x rays vary with filling between $\rho = 1.18$ and $\rho = 1.26$.[25,23] Compare this with $\rho = 1$ as assumed in Fig. 5.

Essentially, the phase diagram does contain only four different phases, namely the solid phases δ and ϵ or ζ and their fluid counterparts liquid and θ, respectively. Melting of the solid phase δ $(0 \leqq \rho \leqq 1)$ does result into an isotropic liquid while melting of the solid phase δ $(1 \leqq \rho \leqq 1.8)$ and ζ $(\rho \geqq 2.8)$ results in the phase θ. One more information about the details of the solidification process can be obtained by the total susceptibility decrease between the liquid phase and the low-temperature solid phase. This quantity $\Delta\chi = \chi_{\text{liquid}} - \chi_{\text{solid}}$ is shown in Fig. 7 as a function of the coverage ρ. It was evaluated by inserting as χ_{liquid} the susceptibility values taken along the low-temperature limit of existence of the liquid phase. This is identical with the observed susceptibility maximum of Figs. 2 and 6. $\Delta\chi$ comprises the effects of all observed phase transitions between the liquid and the very lowest ordered phase. We do not know to what extent $\Delta\chi$ is falsified by alternate-site adsorption etc. Note, however, that $\Delta\chi$ is the difference of χ_{liquid} and χ_{solid} which both should be falsified in a similar manner by those secondary

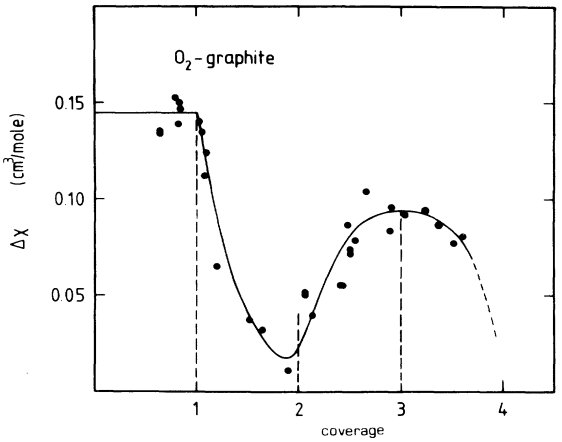

FIG. 7. Decrease of susceptibility due to solidification, $\Delta\chi$, as a function of coverage, ρ. For a discussion, refer to text.

effects. Therefore, the corresponding error may be assumed to cancel more or less.

It can be seen from Fig. 7 that solidification is associated with a constant susceptibility reduction per O_2 molecule in the range $\rho < 1$. In the consecutive range $1 < \rho < 2$ $\Delta\chi$ decreases continuously down to a small value. Since it seems well established that all the observed solid phases have nearly identical susceptibilities we must attribute the strong changes in $\Delta\chi$ to changes within the liquid phase which assumes magnetic properties which become more and more solidlike on going from $\rho = 1$ to $\rho = 1.8$, e.g., liquid$\rightarrow\theta$. This assumption is also supported by the fact that virtually no susceptibility anomaly can be seen for $\rho \simeq 1.8$. Near to this coverage the liquid-solid transition is very gradual and smooth. The specific-heat measurements confirm this result since also this method reveals no melting anomaly just for $\rho = 1.8$.

On going from $\rho = 1.8$ to $\rho = 2.8$ solidification implies an increasing susceptibility change and $\Delta\chi$ for $\rho = 2.8$ again becomes two-thirds of the value of the $\delta\rightarrow$liquid transition at $\rho \simeq 1$. We interpret this as critical behavior that gradually reappears in the corresponding range of coverage. The reappearance is accompanied by χ anomalies which, due to growing coverage, become steeper and steeper until a coverage is reached where the θ phase or the θ' phase, respectively (refer to Figs. 2 and 6) become reestablished. With further increasing O_2 density those θ and θ' phases again become more and more solidlike which is anticipated to be accompanied by a decreasing $\Delta\chi$. This is in fact observed in Fig. 7.

IV. PARAMAGNETIC ORDERING TEMPERATURE OF THE LIQUID PHASE

It is interesting to do one more analysis with the $\chi(T)$ results in order to get information about the density dependence of the paramagnetic ordering temperature of the liquid phase.

For this we have analyzed the susceptibility in the limited temperature interval of $30 < T < 60$ K by fitting a Curie-Weiss law $\chi = C/(T - \Theta)$ to the experimental $\chi(T)$ curves. Note that the data used for this analysis are always restricted to the liquid phase. The problem in achieving a reliable fit from which an approximate value of the Curie-Weiss temperature can be determined is the correct subtraction of the background susceptibilities due to quartz container and Grafoil substrate. These susceptibility contributions turned out to be not in exact proportionality to the weight of quartz and Grafoil probably due to somewhat different dimensions of the quartz containers which accordingly sample different field gradients when exceeding the range of best field homogeneity of the magnetometer. The background susceptibility is therefore determined for each sample individually such that the slope of the Curie-Weiss law does correspond to the number of O_2 molecules in the sample. As a result of the very limited temperature interval over which the Curie-Weiss law can be followed the obtained Θ values do scatter strongly. Figure 8 shows that all Θ values are negative and that Θ increases with increasing O_2 content indicating stronger antiferromagnetic interactions, viz., rotational hindering potentials in the liquid phase for higher O_2 densities. The quantitative results of Fig. 8 are subject to considerable experimental uncertainties and should therefore not be overestimated. However they indicate rather

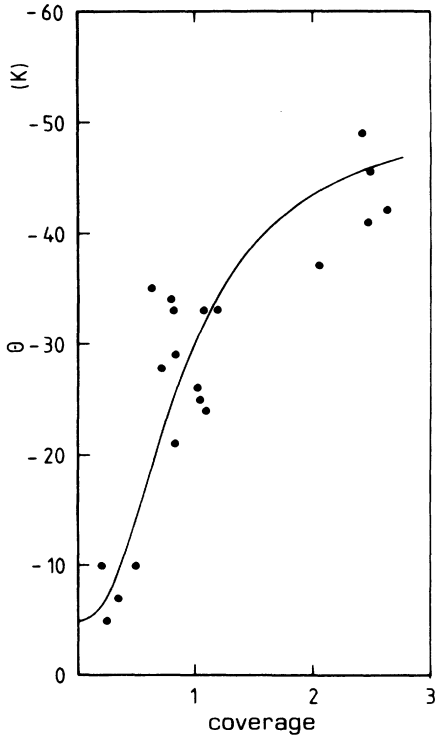

FIG. 8. Paramagnetic ordering temperature Θ as a function of O_2 density ρ evaluated for the liquid phase. The smooth line is used as a guide to the eye.

well the increasing O_2-O_2 interaction as it is also displayed by the salient features of the phase diagram which only at the higher coverages exhibits phase structures with antiferromagnetic order.

V. CONCLUSIONS

A detailed susceptibility study of the melting process of 2D O_2 physisorbed on Grafoil has enabled us to give a more complete view of the phase diagram of this system. The proposed phase diagram includes all phase transitions hitherto known but allows conclusive interpretation of some additional features which were not well understood until now, such as the observed double structure in the specific heat observed only very near to $\rho \simeq 1$ and the change from a δ-type anomaly at $\simeq 25$ K for $\rho < 1$ to a λ-type anomaly at $T \simeq 32$ K for $\rho > 1$. The susceptibility measurements led us to conclude with the existence of a new type of fluid characterized by properties which are very similar to the solid phase. A final confirmation of all details in the O_2-graphite phase diagram requires further experimental efforts preferentially by using surface-sensitive scattering techniques in order to resolve the two different types of fluid phases.

ACKNOWLEDGMENTS

We acknowledge the support afforded by Professor E. F. Wassermann and Professor W. Zinn to this work. Thanks are also extended to R. Braun and B. Christoffer for sample preparation, F. Deloie and H. J. Bierfeld for valuable assistance in sample measurement and analysis, respectively.

---

*Present address: Medizinische Einrichtungen der Universität Köln, D-5 Köln 41, Kerpener Strasse 32.

[1]S. Gregory, Phys. Rev. Lett. **40**, 723 (1978).
[2]D. D. Awschalom, G. N. Lewis, and S. Gregory, Phys. Rev. Lett. **51**, 586 (1983).
[3]M. Nielsen and J. P. McTague, Phys. Rev. B **19**, 3096 (1979).
[4]P. W. Stephens, P. A. Heiney, R. J. Birgeneau, P. M. Horn, J. Stoltenberg, and O. E. Vilches, Phys. Rev. Lett. **45**, 1959 (1980).
[5]P. A. Heiney, P. W. Stephens, S. G. J. Mochrie, J. Akimitsu, R. J. Birgeneau, and P. M. Horn, Surf. Sci. **125**, 539 (1983).
[6]M. F. Toney, R. D. Diehl, and S. G. Fain, Jr., Phys. Rev. B **27**, 6413 (1983).
[7]R. Marx and R. Braun, Solid State Commun. **33**, 229 (1980).
[8]J. Stoltenberg and O. E. Vilches, Phys. Rev. B **22**, 2920 (1980).
[9]R. Marx and B. Christoffer, Phys. Rev. Lett. **51**, 790 (1983).
[10]P. W. Stephens, R. J. Birgeneau, C. F. Majkrzak, and G. Shirane, Phys. Rev. B **28**, 452 (1983).
[11]R. J. Meier and R. B. Helmholdt, Phys. Rev. B **29**, 1387 (1984).
[12]R. Marx and B. Christoffer, unpublished results.
[13]D. R. Nelson and B. I. Halperin, Phys. Rev. B **19**, 2457 (1979); S. Ostlund and B. I. Halperin, *ibid.* **23**, 335 (1981); J. M. Kosterlitz and D. J. Thouless, J. Phys. C **6**, 1181 (1973).
[14]G. Herzberg, *Molecular Spectra and Molecular Structure, I. Spectra of Diatomic Molecules* (van Nostrand Reinhold, New York, 1950).
[15]J. G. Dash, *Films on Solid Surfaces* (Academic, New York, 1975).
[16]G. C. De Fotis, Phys. Rev. B **23**, 4714 (1981).
[17]J. Dericbourg, Surf. Sci. **59**, 554 (1976).
[18]J. G. Dash and R. D. Puff, Phys. Rev. B **24**, 295 (1981); R. E. Ecke, J. G. Dash, and R. D. Puff, *ibid.* **26**, 1288 (1982).
[19]Y. Imry, Phys. Rev. B **21**, 2042 (1980); M. E. Fisher and A. N. Berker, *ibid.* **26**, 2507 (1982); V. Privman and M. E. Fisher, J. Stat. Phys. **33**, 385 (1983); K. Binder and D. P. Landau, Phys. Rev. B **30**, 1477 (1984); M. S. S. Challa, D. P. Landau, and K. Binder, *ibid.* **34**, 1841 (1986); M. E. Fisher and V. Privman, *ibid.* **32**, 447 (1985).
[20]S. C. Fain, Jr., M. F. Toney, and R. D. Diehl, in *Proceedings of the Ninth International Vacuum Congress and Fifth International Conference on Solid Surfaces,* edited by J. L. de Segovia (Imprenta Moderna, Madrid, 1983), pp. 129–137.
[21]M. Bienfait, J. L. Seguin, J. Suzanne, E. Lerner, J. Krim, and J. G. Dash, Phys. Rev. B **29**, 983 (1984).
[22]M. Drir and G. B. Hess, Phys. Rev. B **33**, 4758 (1986).
[23]H. You and S. C. Fain, Jr., Phys. Rev. B **33**, 5886 (1986).
[24]R. D. Etters and O. B. M. Hardouin Duparc, Phys. Rev. B **32**, 7600 (1985).
[25]S. C. Fain, Jr. (private communication).
[26]R. Marx, Phys. Rep. **125**, 1 (1985).